

Short communication

4-Bromobenzyl isocyanate versus benzyl isocyanate—New film-forming electrolyte additives and overcharge protection additives for lithium ion batteries

C. Korepp^a, W. Kern^b, E.A. Lanzer^a, P.R. Raimann^a, J.O. Besenhard^a,
M. Yang^c, K.-C. Möller^a, D.-T. Shieh^c, M. Winter^{a,*}

^a Institute for Chemistry and Technology of Inorganic Materials, Graz University of Technology, Stremayrgasse 16, A-8010 Graz, Austria

^b Institute for Chemistry and Technology of Organic Materials, Graz University of Technology, Stremayrgasse 16, A-8010 Graz, Austria

^c Materials Research Laboratories ITRI, Chutung, Hsin-Chu, Taiwan 310, ROC

Available online 28 June 2007

Abstract

Electrochemical properties and working mechanisms of benzyl isocyanate compounds as polymerizable electrolyte additives for overcharge protection of lithium ion batteries have been studied by cyclic voltammetry, charge–discharge cycling, overcharge tests, accelerating rate calorimetry (ARC) and in situ Fourier transform infrared spectroscopy (FTIRS). The overcharge and FTIRS data clearly reveal that 4-bromobenzyl isocyanate (Br-BIC) can electrochemically polymerize at 5.5 V (versus Li/Li⁺) to form an overcharge-inhibiting (probably insulating) film on the cathode surface. In addition, it is found the Br-BIC does slightly improve the charge/discharge performance of a lithium ion battery. Furthermore, Br-BIC and benzyl isocyanate show beneficial solid electrolyte interphase (SEI) formation behaviour on graphite in propylene carbonate based electrolyte solutions. © 2007 Elsevier B.V. All rights reserved.

Keywords: Lithium ion batteries; Electrolyte additives; Solid electrolyte interphase (SEI); In situ FTIR; Overcharge; Isocyanates

1. Introduction

Lithium ion batteries (LIBs) show high energy density, high power capability, high voltage and light weight. Unfortunately, safety of LIBs is still an issue, as for instance overcharge and cell heating may lead to thermal runaway and eventually cell fire and explosion [1–6].

Lithium ion cells may emit smoke, fire or even explode when abused. Upon heating, several exothermic reactions occur inside the cell. Many factors can be possible triggers of cell heating, including external and internal shorts and dropping or crushing of cells. It is generally considered that “thermal runaway” occurs if heat output in the cell exceeds heat dissipation from the cell to the environment. Possible exothermic reactions are: reduction of the electrolyte by the anode, thermal decomposition of the solid electrolyte interphase (SEI) [7], oxidation of the electrolyte at the cathode [8], decomposition of the anode and reaction of

the anode with the electrolyte [9], reaction of the binder and thermal decomposition of the binder [10], and decomposition of the cathode and reaction with the electrolyte [11].

When cells are overcharged [1], the lithium ions remaining in the cathode Li_{0.5}CoO₂ (after full standard charging) are removed at >4.3 V. On the cathode side the Li_{0.5-x}CoO₂ structure collapses during further removal, which is accompanied by oxygen release and impedance increase, whereas at the anode side, excess lithium ions are supplied to the carbon anode [1,12]. When the lithium insertion ability of the carbon anode has exceeded, lithium metal may be deposited on the carbon surface. In parallel to lithium de-insertion from the cathode also electrolyte oxidation occurs, contributing to impedance increase and accumulation of gaseous electrolyte decomposition products. The higher the cathode potential, the higher is the relative share of electrolyte oxidation to the overall overcharge reactions. All these processes finally endanger cell thermal stability and thus cell safety.

To limit or prevent overcharge, many measures can be applied. Well-known approaches are electrolyte additives [13]: (I) certain additives can activate the pressure-sensitive current intermittent device (CID) of a cell as they evolve gas under

* Corresponding author.

E-mail addresses: DTShieh@itri.org.tw (D.-T. Shieh),
martin.winter@tugraz.at (M. Winter).

overcharge. This group of additives comprises cyclohexylbenzene or cyclopentylbenzene (evolving H_2 upon overcharge) [14], pyrocarbonates (evolving CO_2) [15] and biphenyl derivatives (evolving H_2) [16,17]. (II) The redox shuttle approach for overcharge protection uses electrolyte additives, which are activated during overcharge and then act as internal current shunt. These shuttle compounds include, e.g. *n*-butylferrocene [18], tricyanobenzene, tetracyanoquinodimethane, Na salts of 1,2,4-triazole and imidazole [19,20] and Li salts of the formula $Li_2B_{12}F_{12-x}H_x$ [21].

Here, we investigate the aromatic isocyanate compounds benzyl isocyanate (BIC) and 4-bromobenzyl isocyanate (Br-BIC) as overcharge protection additives.

2. Experimental

Propylene carbonate (Honeywell, battery grade), $LiClO_4$ (Mitsubishi Chemical Corp., battery grade), benzyl isocyanate (ALDRICH, 99%) and 4-bromobenzyl isocyanate (ALDRICH, 98%) have been used as received without further purification. The “standard” electrolytes were 1 M $LiPF_6/EC:DMC$ (v:v, 1:1, Merck) and 1 M $LiPF_6/EC:EMC$ (v:v, 1:2, Mitsubishi Chemical Corp.). EC: ethylene carbonate, DMC: dimethyl carbonate, and DEC: diethyl carbonate. The electrode materials consisted of mesocarbon microbeads (MCMB 1028, Osaka Gas), $LiCoO_2$ (Nippon Chemical), Graphite TIMREX KS6 (TIMCAL) and polyvinylidene fluoride/hexafluoropropylene (PVDF/HFP) binder (Kureha Chemical). The carbon electrodes contained 90 wt.% MCMB and 10 wt.% PVDF/HFP. The $LiCoO_2$ electrodes contained 90 wt.% $LiCoO_2$, 5 wt.% KS6 and 5 wt.% PVDF/HFP. Electrolyte preparation and cell assembly have been accomplished under dry Ar in a glove box. A 3-electrode single compartment cell was used for the cyclic voltammetric experiments. Li metal was used for both counter and reference electrode. Cyclic voltammetry has been performed with a laboratory-made potentiostat (Adesys[®]) with a scan rate of $50 \mu V s^{-1}$ in the potential range respectively 3000–4200 versus Li/Li^+ . For constant current cycling, the square electrode design of the anode was $2.5 \text{ cm} \times 2.5 \text{ cm}$. The square electrode design of the cathode was $2 \text{ cm} \times 2 \text{ cm}$. The anode/cathode capacity ratio was 1.151. The theoretical capacity for this full cell design was 4.5 mAh. Celgard[®] 2400 was drenched in a 200 μl electrolyte. Charge/discharge cycling at a defined rate of C/10 has been performed with the Adesys[®] potentiostat/galvanostat.

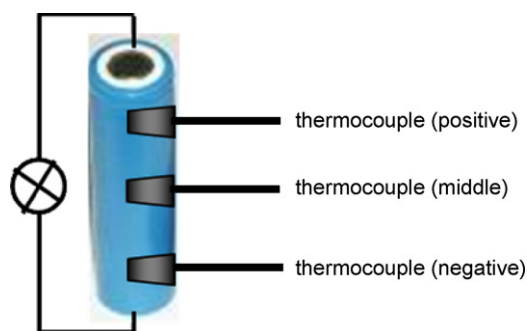


Fig. 1. Locations of the three thermocouples in the 18,650 cell.

For accelerating rate calorimeter (ARC) experiments, 18,650 cells (MCMB//Celgard[®]2400 separator+ electrolyte// $LiCoO_2$) have been assembled. Cells were charged by constant current (1 C) to 4.2 V^+ , then disconnected and transferred to the ARC. Tests were carried out in a closed container (with a pressure line equipped with the sample gas collection cylinders having a total volume near 10 l). A rest time of 100 min was used to accomplish thermal equilibration of the battery. A heating rate of $5 \text{ }^\circ\text{C min}^{-1}$ within 90–300 $^\circ\text{C}$. was applied. The onset of exothermic reactions was defined as the time when the self-heating rate (SHR) is $>0.02 \text{ }^\circ\text{C min}^{-1}$.

Overcharge tests were performed with Maccor Battery Testing Equipment using 18,650 cells, assembled as described above. After pre-galvanostatic charge to 4.2 V at 0.1 C the cells were overcharged galvanostatically at a rate of 1 C–6.5 V followed by constant voltage charge at 6.5 V for at least 5 h. The tests were performed without a PTC overcharge protection device. The temperature changes are monitored by three thermocouples in the cell (Fig. 1).

In situ FTIR experiments have been performed in a self-made IR-cell described elsewhere [22] The cell has been provided with an optical CaF_2 window. The working electrode was a 12 mm diameter glassy-carbon electrode (GC) as GC has a good capability for IR beam reflection. Metallic Li was used as reference and counter electrode.

3. Results

3.1. Cyclic voltammetry and constant current cycling

If effective solid electrolyte interphase (SEI) film formation does not take place co-intercalation and subsequent reduction of

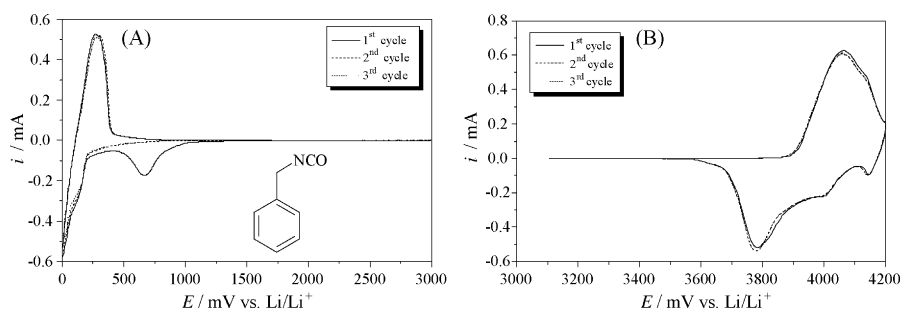


Fig. 2. Cyclic voltammograms of a MCMB graphite electrode (A) and a $LiCoO_2$ electrode (B) in 2 wt.% BIC in 1 M $LiClO_4/PC$, scan rate: $50 \mu V s^{-1}$.

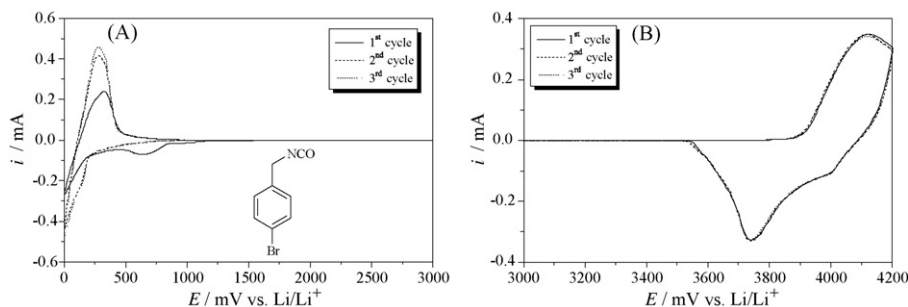


Fig. 3. Cyclic voltammograms of a MCMB graphite electrode (A) and a LiCoO₂ electrode (B) in 2 wt.% Br-BIC in 1 M LiClO₄/PC, scan rate: 50 μV s⁻¹.

PC results in heavy gassing and thus exfoliation of graphite. Both benzyl isocyanates are able to act as film-forming electrolyte additive and thus to diminish PC co-intercalation.

Benzyl isocyanate (BIC) belongs to the class of benzyl isocyanates and features a benzyl ring with the electron-withdrawing isocyanate group in β-position. The cyclic voltammogram (Fig. 2) shows that BIC is reduced at ~1.25 V versus Li/Li⁺. At the LiCoO₂ composite electrode, no substantial additive oxidation occurs.

4-Bromo-benzyl isocyanate (Br-BIC), has been selected to study the influence of an electron-withdrawing benzyl substituent, e.g. bromine. The reduction of Br-BIC in PC starts also at ~1.25 V versus Li/Li⁺ (Fig. 3). The difference in Li intercalation/de-intercalation currents between the first and later cycles should be noted. Compared to Br-BIC, BIC causes larger reduction currents (1.25 V versus Li/Li⁺) indicating that BIC is a less effective additive. At LiCoO₂, Br-BIC additive oxidation occurs, moreover, lithium de-intercalation and intercalation peaks are not that well resolved. However, no significant changes in the current peak shapes can be observed.

In 2-electrode pouch bag cells with an EC:DMC standard electrolyte (Fig. 4) BIC and Br-BIC seem to improve the cell performance compared to the electrolyte without additive.

3.2. Accelerating rate calorimetry

ARC revealed that the isocyanate additives had some positive influence on the SEI thermal stability, but did finally deteriorated the full cell thermal stability.

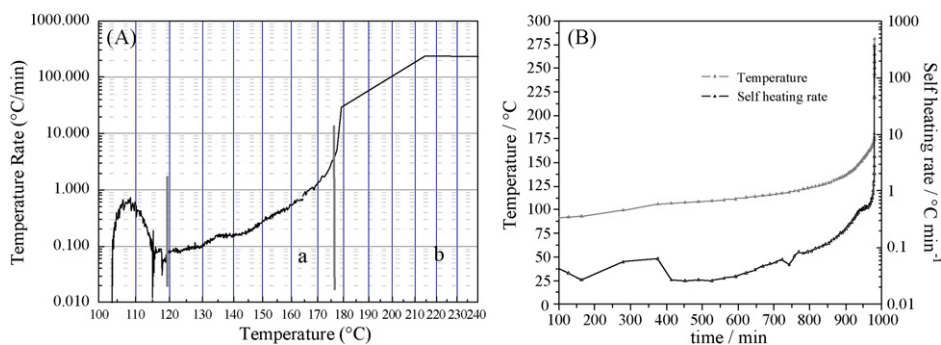


Fig. 5. (A) ARC profile of a 800 mAh 18,650 Li-ion cell: MCMB anode, LiCoO₂ cathode, Celgard 2400 separator, 1 M LiPF₆/EC:EMC (v:v, 1:2), open-circuit potential at 4.2 V, under adiabatic conditions. (a) Self-heating region prior to thermal runaway, and (b) thermal runaway region. (B) Temperature and self-heating rate (SHR) vs. time.

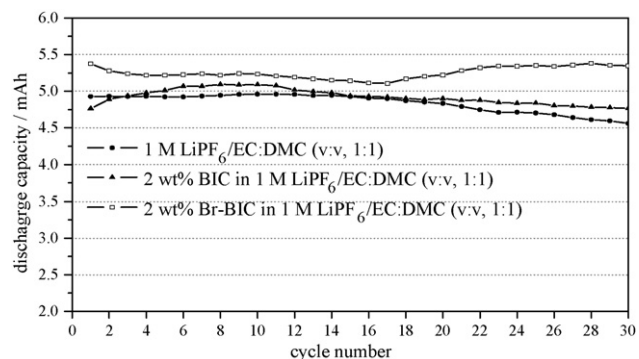


Fig. 4. Discharge capacities of MCMB/LiCoO₂ pouch bag cells using 1 M LiPF₆/EC:DMC (v:v; 1:1) electrolytes with and without 2 wt.% Br-BIC and BIC as additives under 1 C constant current cycling, cut-off: 4.2–2.8 V.

Fig. 5A showing the ARC profile (self-heating rate (SHR) versus temperature) demonstrates that small self-heating, probably due to SEI decomposition, starts at ~120 °C but is not self-sustaining. The next heating area (a) shows slow self-heating to ~175 °C. Thermal runaway can be observed in the area (b). Fig. 5B shows the SHR and temperature profile plotted versus time. Within 1000 min, the cell temperature increases up to ~300 °C, during thermal runaway.

Fig. 6A shows an ARC profile under the same experimental conditions except for the presence of 2 wt.% of the electrolyte additive BIC. Self-heating exothermic reactions start at ~115 °C (SEI decomposition). The heating region (a) starts ~5 °C earlier (cf. Fig. 5) and shows self-heating up to ~180 °C, when thermal runaway (area b) occurs. Finally, the

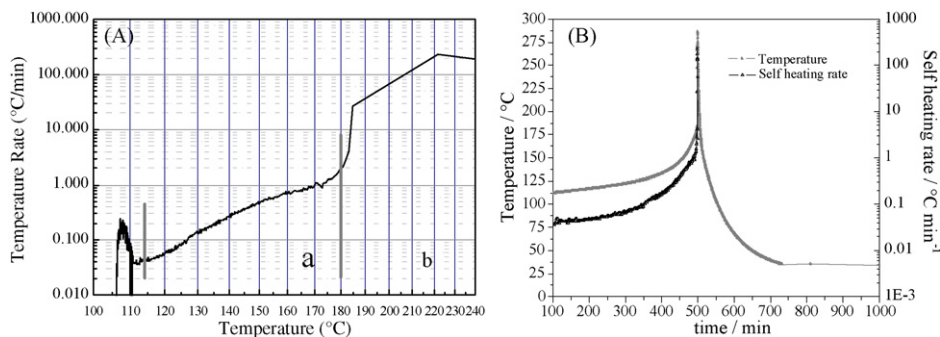


Fig. 6. (A) ARC profile of a 800 mAh 18,650 Li-ion cell: MCMB anode, LiCoO₂ cathode, Celgard 2400 separator, 2 wt.% BIC in 1 M LiPF₆/EC:EMC (v:v, 1:2), open-circuit potential at 4.2 V, under adiabatic conditions. (a) Self-heating region prior to thermal runaway, and (b) thermal runaway region. (B) Temperature and self-heating rate (SHR) vs. time.

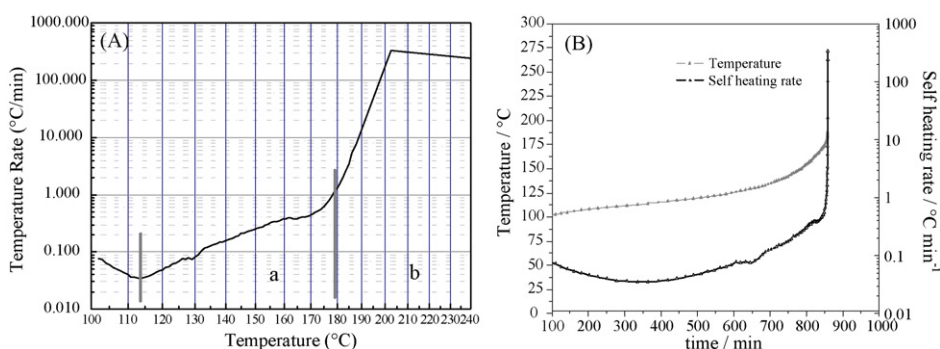


Fig. 7. (A) ARC profile of a 800 mAh 18,650 Li-ion cell: MCMB anode, LiCoO₂ cathode, Celgard 2400 separator, 2 wt.% Br-BIC in 1 M LiPF₆/EC:EMC (v:v, 1:2), open-circuit potential at 4.2 V, under adiabatic conditions. (a) Self-heating region prior to thermal runaway, and (b) thermal runaway region. (B) Temperature and self-heating rate (SHR) vs. time.

cell temperature increases up to ~ 300 °C after already ~ 500 min (Fig. 6B), which is half time compared to the standard electrolyte (Fig. 5B).

The last ARC profile (Fig. 7A) is that of a 18,650 cell containing the electrolyte with 2 wt.% Br-BIC as additive. SEI decomposition does not seem to occur in the range of 100–120 °C, indicating a thermal reinforcement of the SEI by Br-BIC. The self-heating area (a) starts ~ 5 °C earlier than with the standard electrolyte and shows slow self-heating up to ~ 180 °C, when thermal runaway starts Fig. 7B reveals that the cell temperature during thermal runaway increases until ~ 275 °C. Thermal runaway starts after ~ 850 min, i.e. again earlier than with the standard electrolyte.

3.3. Overcharge tests

The overcharge test with the 18,650 cell containing the standard electrolyte (Fig. 8) results in thermal runaway. The cell temperature goes up to ~ 500 °C and the cell starts to smoke and to fire afterwards. The rate of voltage-increase varies during the test, indicating different (and probably at least partially subsequent) overcharge reaction mechanisms. Cell current and voltage broke down due to the destruction of experimental setup, which determines the end of the test.

The addition of 2 wt.% of the respective isocyanates has very different effects on the overcharge behaviour. With the BIC addi-

tive (Fig. 9), the cell temperature went up to >800 °C and the cells started to smoke and to detonate afterwards. Again current and voltage broke down by cell destruction. BIC does not have a positive impact on the overcharge behaviour.

With Br-BIC (Fig. 10), the cell temperature increases, but can be kept always below ca. 80 °C. First rapidly increasing (with a small plateau at 5.5 V), the voltage finally remains constant at ~ 7 V for $>14,000$ s, when the test was stopped. In parallel, the temperature went rapidly down to 20 °C.

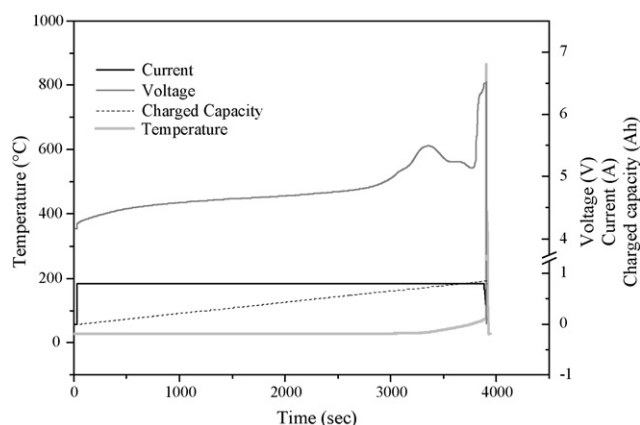


Fig. 8. Overcharge test of a 800 mAh 18,650 Li-ion cell: MCMB, LiCoO₂, Celgard 2400, 1 M LiPF₆/EC:EMC (v:v, 1:2), charged to 6.5 V.

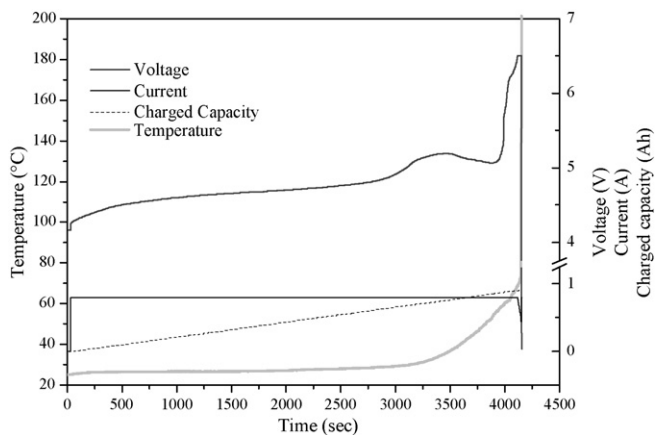


Fig. 9. Overcharge test of a 800 mAh 18,650 Li-ion cell: MCMB, LiCoO₂, Celgard 2400, 2 wt.% BIC in 1 M LiPF₆/EC:EMC (v:v, 1:2), charged to 6.5 V.

3.4. In situ FTIR spectroscopy

To understand the different overcharge behaviour of BIC and Br-BIC, we have performed in situ FTIR measurements with a glassy-carbon (GC) electrode in the potential range from 3.0 to 7.0 V versus Li/Li⁺. With regard to GC as model electrode for the composite LiCoO₂ electrode, it should be noticed, that the composite electrode contains carbon as additive, which is a very conductive part of the electrode, allowing the assumption that a significant fraction of electrolyte oxidation reaction takes part on the carbon additive.

Fig. 11 gathers the spectra of the electrolyte with Br-BIC as additive: Clearly visible is an IR band at ~2275 cm⁻¹ representing the asymmetric –NCO stretching vibration of isocyanate compounds. This band decreases, indicating that the –NCO functional group of Br-BIC takes part in the electrochemical process. In parallel, new bands appear at 1300–1600 cm⁻¹. The band at 1580 cm⁻¹ can be assigned to a N–H deformation vibration and indicates incorporation of isocyanate compounds into a polymeric network. The band appearing at 1632 cm⁻¹ is assigned to a “C–CO–NR₂-group in the solid state” and indicates that a solid product is formed on the glassy-carbon surface during oxidation. Other band changes in the spectra can be

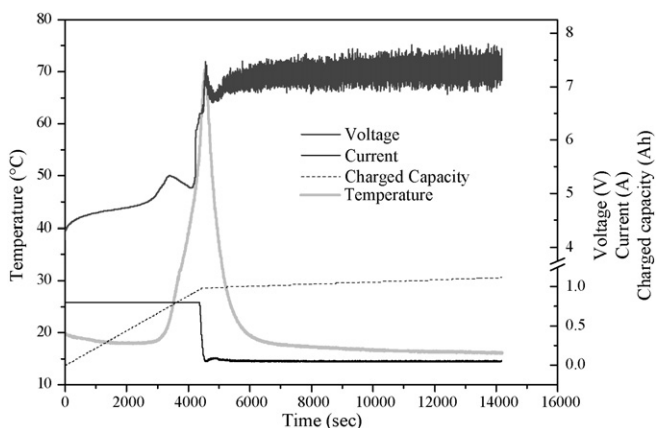


Fig. 10. Overcharge of a 800 mAh 18,650 Li-ion cell: MCMB, LiCoO₂, Celgard 2400, 2 wt.% Br-BIC in 1 M LiPF₆/EC:EMC (v:v, 1:2), charged to 6.5 V.

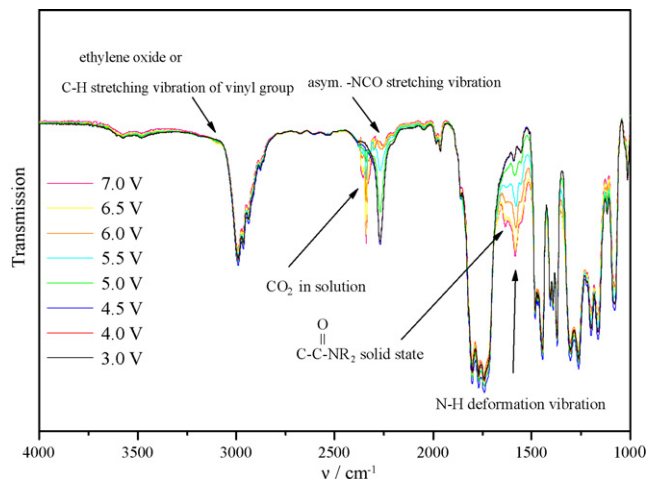


Fig. 11. Transmission FTIR spectra of 10 vol.% Br-BIC in 1 M LiPF₆/EC:EMC (1:2; v:v) at a glassy-carbon electrode during overcharge to 7.0 V vs. Li/Li⁺.

Table 1

Assignment of infrared bands in the FTIR spectra in Figs. 11 and 12, related to the oxidation of 1 M LiPF₆ in EC [23–25]

Wavenumber (cm ⁻¹)	Assignment
2995, 2930	C–H stretching vibration
1860, 1825, 1790, 1760	C=O stretching vibration
1195, 1150, 1065	C–O–C–O–C skeletal vibration

assigned to oxidation of the base electrolyte 1 M LiPF₆/EC:EMC and interpreted with the help of literature data (Table 1, Fig. 12). For EC, it has been concluded, that the first step in the oxidation is ring opening, which is followed by polymerization, thus formation of polymeric products on the cathode surface. In parallel CO₂ is evolved (band at 2343 cm⁻¹). Our spectra confirm that EC is decomposed by oxidation. In addition, we observed that the achromatic electrolyte turned into a brown colour after the electrochemical experiment. This might be due to dissolved Br₂ formed by oxidation of Br-BIC.

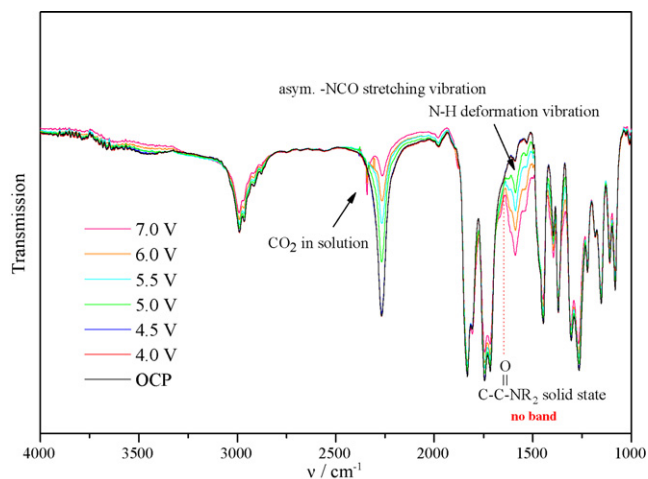


Fig. 12. Transmission FTIR spectra of 10 vol.% BIC in 1 M LiPF₆/EC:EMC (1:2; v:v) at a glassy-carbon electrode during overcharge to 7.0 V vs. Li/Li⁺.

In summary, we can conclude that Br-BIC is an electrolyte additive, which starts to polymerize on the cathode surface during overcharge >5 V versus Li/Li⁺ (cf. the small voltage plateau at 5.5 V in Fig. 10). The formed polymer stops the overcharge reaction. It is assumed that the Br-BIC monomer polymerization proceeds via radical anions. The intermediates may react with (i) other isocyanate monomers, resulting in polymerized products, e.g. polyimides, which participate in the surface film and/or (ii) with other electrolyte components (LiPF₆, EC or EMC) which participate in the electrolyte oxidation process by subsequent and/or parallel reactions. The oxidation of Br⁻ to elemental Br₂ might trigger the decomposition/polymerization reaction of Br-BIC.

As was expected, the in situ FTIRS analysis of the BIC additive yielded different results. Compared to Br-BIC, the band at ~ 2275 cm⁻¹ (asymmetric -NCO stretching vibration) does not decrease as strongly and is still visible at 7 V versus Li/Li⁺. Furthermore, the band at 1632 cm⁻¹, assigned to C-CO-NR₂ in the solid state, is absent. We thus conclude, that BIC is not forming a polymer film on the GC electrode surface. Furthermore the electrolyte remains colourless, as there is no Br-source in the electrolyte. The bands due to EC oxidation may be assigned as has been done for Br-BIC (Table 1). In general, the results are in agreement with the overcharge test, where BIC had no protection effect.

4. Conclusion

Two benzyl isocyanate, benzyl isocyanate (BIC) and 4-bromo-benzylisocyanate (Br-BIC) compounds have been investigated for their use as electrolyte additives in lithium ion batteries. Both additives are able to suppress PC co-intercalation into graphite and also improve the cycling behaviour of MCMB/LiCoO₂ cells, even when only present in small amounts of 2 wt.% in a 1 M LiPF₆/EC:DMC electrolyte.

In addition, the isocyanate compounds were checked with regard to protection versus thermal runaway or overcharge in 18,650 full cells with MCMB anode, LiCoO₂ cathode and 1 M LiPF₆/EC:EMC electrolyte. ARC results showed that the full cells with the isocyanate compounds experienced thermal runaway faster than the cell with the standard electrolyte. In an overcharge test, however, the presence of only 2 wt.% Br-BIC stopped thermal runaway and consequently cell fire and explosion, whereas thermal runaway was observed in the electrolyte without additives or with the additive BIC. To understand the different results: in the ARC experiment, self-heating is induced by external heating. In the overcharge experiment, heating is induced by electrochemical measures. Br-BIC is obviously only effective via electrochemical and not via thermal activation. To get a deeper insight in the modus operandi of Br-BIC as overcharge protection additive, in situ FTIRS was applied. Results

proved that Br-BIC forms a polymeric film on the electrode surface, during overcharge. The polymerization reaction starts at a cell voltage >5 V. Such a polymer film is not observed in the presence of BIC, indicating the importance of the oxidation-sensitive Br-functionality in the Br-BIC additive.

Acknowledgements

We thank Honeywell (Seelze, Germany), Merck (Darmstadt, Germany) and Mitsubishi Chemical Corp. (Tsukuba, Japan) for supplying samples used in this study.

References

- [1] S. Tobishima, J. Yamaki, *J. Power Sources* 81–82 (1999) 882.
- [2] S. Passerini, F. Coustier, B.B. Owens, *J. Power Sources* 90 (2000) 144.
- [3] Ph. Biensan, B. Simon, J.P. Peres, A. de Guibert, M. Broussely, J.M. Bodet, F. Pertion, *J. Power Sources* 81–82 (1999) 906.
- [4] K. Kito, H. Nemoto, *J. Power Sources* 81–82 (1999) 887.
- [5] S. Tobishima, K. Takei, Y. Sakurai, J. Yamaki, *J. Power Sources* 90 (2000) 188.
- [6] S. Tobishima, Y. Sakurai, J. Yamaki, *J. Power Sources* 68 (1997) 455.
- [7] U. von Sacken, J.R. Dahn, in: *Extended Abstracts of Electrochemical Society Fall Meeting*, WA, USA, 1990, p. 87.
- [8] M.A. Gee, F.C. Laman, *J. Electrochem. Soc.* 140 (1993) L53.
- [9] F.C. Laman, Y. Sakurai, T. Hirai, J. Yamaki, S. Tobishima, in: *Extended Abstracts of Sixth International Meeting on Lithium Batteries*, Munster, Germany, 1992, p. 298.
- [10] D. Fouchard, L. Xie, W. Ebner, S. Megahead, *Proc. Symp. Rechargeable Lithium and Lithium-Ion Batteries*, The Electrochem. Soc. Inc., NY, USA, 1994, p. 348.
- [11] Z. Zhang, in: *Extended Abstracts of 9th International Meeting on Lithium Batteries*, Edinburgh, Scotland, UK, abstract Anode I, Oral 6, 1998.
- [12] S. Tobishima, K. Takei, Y. Sakurai, J. Yamaki, *J. Power Sources* 90 (2000) 185.
- [13] G.E. Blomgren, *J. Power Sources* 199–121 (2003) 326.
- [14] M. Takahashi, Z. Yasutake, K. Abe, A. Ueki, T. Hamamoto, Sanyo, Ube, US Pat. No. 6,632,572 (2003).
- [15] N. Sugeno, Sony, US Pat. No. 5,427,874 (1995).
- [16] H. Mao, U. von Sacken, Moli Energy, US Pat. No. 5,776,627 (1998).
- [17] J.N. Reimers, B.M. Way, E-One Moli Energy, US Pat. No. 6,074,777 (2000).
- [18] K.M. Abraham, D.M. Pasquariello, E.B. Willstädt, *J. Electrochem. Soc.* 137 (1999) 1856.
- [19] T.J. Richardson, P.N. Ross, *J. Electrochem. Soc.* 143 (1996) 3992.
- [20] T.J. Richardson, P.N. Ross, US Dept. of Energy, USA, US Pat. No. 6,004,698 (1999).
- [21] W. Casteel, *Proceedings of the 1st International Symposium on Large Lithium Ion Battery Technology and Application (LLIBTA), Fifth Advanced Automotive Battery Conference (AABC-05)*, Honolulu (Hawaii), June 12–17 (2005).
- [22] K.-C. Möller, H.J. Santner, W. Kern, S. Yamaguchi, J.O. Besenhard, M. Winter, *J. Power Sources* 119–121 (2003) 561.
- [23] F. Joho, P. Novak, *Electrochim. Acta* 45 (2000) 3589.
- [24] R.A. Nyquist, W.J. Potts, *Spectrochim. Acta* 17 (1961) 679.
- [25] Standard Spectra Collection, Sadtler Research Laboratories, Philadelphia, PA, USA.